# HEART RATE REDUCTION IMPROVES BIVENTRICULAR FUNCTION AND INTERACTIONS IN EXPERIMENTAL PULMONARY HYPERTENSION

Olga Gomez (1), Kenichi Okumura (1), Osami Honjo (1), Mei Sun (1), Ryo Ishii (1), Bart Bijnens (2, 3)*, and Mark K. Friedberg (1)*.

1-The Labatt Family Heart Center. Division of Cardiology and Cardiovascular Surgery. Hospital for Sick Children and University of Toronto, Canada**.**

2-ICREA, Barcelona, Spain.

3-Department of information and Communication Technologies, Universitat Pompeu Fabra, Barcelona, Spain.

* Co-senior authors. All authors have contributed to the manuscript as detailed below: experimental design (KO, OH MS, MF), echocardiography (KO and RI), echo measurements (OG and RI), conception, design, supervision and revision for intellectual content (MF and BB). All the authors have contributed to the interpretation of the data and have approved the final version of the manuscript.

No relationships with industry.

**Short title:** Heart rate reduction impact on pulmonary hypertension.

Corresponding author:

Mark K. Friedberg, MD

Division of Cardiology, Hospital for Sick Children

555 University Avenue, Toronto, Ontario M5G 1X8

Phone: 416-813-7239, Fax: 416-813-7547, email: mark.friedberg@sickkids.ca

**Word count: 6318**

**This research was supported by a grant from the Canadian Heart and Stroke Foundation**

## ABSTRACT

**Objectives:** To investigate mechanisms of heart rate (HR) reduction on biventricular function and interactions in experimental pulmonary arterial hypertension (PAH).

**Methods:** We compared cardiac-cycle mechanics and interventricular interactions in 15 sham, 8 monocrotaline-PAH, 9 PAH+carvedilol and 8 PAH+ivabradine rats. We used echocardiography to assess biventricular function, timing of cardiac- cycle events and septal position in PAH rats; and related HR reduction effect on biventricular function measured by echocardiography and conductance catheter.

**Results:** HR was 302 in PAH+carvedilol , 303 in PAH+ivabradine vs. 359 bpm in PAH ($p<0.01$, respectively). Shams showed temporal alignment between right (RV) and left ventricular (LV) events; while PAH-rats showed increased biventricular isovolumic contraction times (ICT), delayed RV peak-radial motion and impaired early relaxation. Temporal malalignment was associated with decreased tricuspid and mitral diastolic annular peak velocities ($E´$) (3.7 vs. 6.4 and 3.4 vs. 5.3, $p<0.001$ respectively), delayed and shortened biventricular filling and reduced early-diastolic LV- filling (E) velocity (0.56 vs. 0.81, $p<0.01$). LV eccentricity index was increased in systole (2.0 vs. 1.2, $p<0.001$), early-diastole (2.1 vs. 1.1, $p < 0.001$) and end-diastole (1.6 vs. 1.1, $p<0.001$) in PAH vs. shams. HR reduction with carvedilol and ivabradine shortened biventricular ICT, time-to biventricular peak-radial motion, improved RV relaxation and increased early-diastolic LV filling through reduced inter-ventricular interaction and improved timing. These improvements corresponded with enhanced hemodynamics (increased cardiac-output, RV contractility and diastolic relaxation).

**Conclusions:** HR reduction by carvedilol and ivabradine improve biventricular filling and hemodynamics in experimental PAH through re-alignment of RV-LV cardiac-cycle events and improved interventricular interactions.

**KEY WORDS**

Pulmonary hypertension, ivabradine, carvedilol, heart rate reduction, interventricular interactions.

**NEW AND NOTEWORTHY**

Carvedilol improves biventricular function in experimental-PAH but the mechanisms of HR reduction vs. beta-blocker effect are inadequately defined. We demonstrate that reducing HR using either carvedilol or ivabradine ($I_f$ inhibitor without beta-blocker effect), improves RV filling and biventricular hemodynamics through the re-alignment of RV-LV cardiac-cycle events and improved interventricular interactions.

## INTRODUCTION

Right (RV) as well as left (LV) ventricular dysfunction drive mortality in pulmonary hypertension (PAH) (9, 15, 8) . We previously showed that the ratio of RV systolic to diastolic duration (S:D ratio) is increased in PAH children in association with worse exercise tolerance and survival (1). A high S:D ratio in PAH reflects prolonged leftward septal shift by the hypertensive RV and associated reduced LV filling, already compromised by the short diastolic duration; thereby reflecting adverse interventricular interactions (7) . With increasing heart rate (HR), diastole shortens and the S:D ratio increases exponentially; markedly so in PAH patients versus a much smaller change in controls (1,21) . Based on these clinical observations and on prior findings that carvedilol improves RV function in experimental PAH (2, 3) we hypothesized that reducing HR in PAH would prolong diastole and decrease the S:D ratio, and might improve interventricular interactions leading to increased filling. This formed the rationale for studying carvedilol's effects in experimental PAH (15). In that study, we found that carvedilol improved biventricular contractility and relaxation, measured by pressure-volume loops, reduced biventricular fibrosis, increased cardiac output, exercise capacity and a trend towards improved survival (15).

However, the impact of HR reduction on biventricular function, interventricular interactions and timing of events in the cardiac cycle in PAH is incompletely defined; and whether carvedilol improves biventricular function in experimental PAH through HR reduction or through adrenergic receptor blockade remains unknown.

Ivabradine is a selective inhibitor of the sinoatrial inward hyperpolarization-activated current ($I_f$) that reduces HR, without beta-blocker effects and without direct effects on global LV systolic function, coronary flow or pulmonary vascular resistance (22-24). Therefore, ivabradine

constitutes a very good tool to assess the effects of HR reduction on biventricular function in PAH, and to differentiate whether carvedilol´s beneficial effects are due to HR reduction or due to its anti-adrenergic properties. Delineating these effects is important as morbidity and mortality in PAH remain high, therapeutic options limited and beta-adrenergic receptor blockers are relatively contraindicated in this condition (6, 19). We hypothesized that reducing HR improves interventricular interactions in PAH independent of beta-adrenergic blockade. Accordingly, we aimed to investigate the effects of carvedilol and ivabradine on cardiac-intervals and interventricular interactions in a rat model of PAH.

## GLOSSARY

RV= right ventricle
PAH= pulmonary arterial hypertension
LV= left ventricle
S:D ratio= systolic to diastolic ratio
HR= heart rate
ECG=electrocardiogram
ICT= isovolumic contraction time
ET= ejection time
IRT= isovolumic relaxation time
TAPSE= tricuspid annular systolic excursion
MAPSE= mitral annular systolic excursion
IVS= interventricular septum
EC= eccentricity index
ICC= intraclass correlation coefficient for absolute agreement
SERCA2a=sarco-endoplasmic-reticulum-$Ca^{2+}$-ATPase2a

## METHODS:

We analyzed echocardiograms from male Sprague-Dawley monocrotaline-induced PAH rats (Charles River Laboratories, Senneville, Canada) from overlapping groups from previously reported experiment (15). For the purposes of this investigation we excluded 2 PAH rats from the original experiment that had profound terminal bradycardia at echocardiography and studied 3 new animals not included in that experiment. For the current study we additionally studied a group of PAH rats treated with ivabradine. Animal care and experiments were conducted according to institutional Animal Ethic Committee and National Institutes of Health guidelines.

### Experimental Protocol:

The experimental protocol has been described previously (15). Rats were 6-weeks old at protocol onset and randomly assigned to the following groups: (a) Shams: received a single subcutaneous injection of 0.9% saline (1 ml) (b) PAH: received a single subcutaneous injection of monocrotaline (60 mg/kg) to induce PAH, (c) PAH+carvedilol: rats were orally treated with carvedilol (15 mg/kg/day, for 3-weeks) and (d) PAH+ivabradine: rats were orally treated with ivabradine (10mg/kg/d, for 3-weeks), the last two groups starting therapy 2-weeks after monocrotaline injection. Rats were euthanized by cardiac extraction under deep isoflurane 3% anesthesia at the terminal experiment, 5-weeks after the start of the protocol.

### Echocardiography:

Using a Vivid-E9 with 12-MHz phased-array transducer (General Electric, Wauwatosa, WI) under light isoflurane 3% sedation, 2D, M-mode, color and pulsed-Doppler were obtained with simultaneous electrocardiogram (ECG) display from rats surviving to the terminal experiment (5-weeks after the monocrotaline injection). Digital data were analyzed offline (EchoPac, version

8.0, GE). 3-cardiac cycles were analyzed using the ECG R-wave as a reference. Cardiac-cycle duration (RR-interval) and HR were recorded.

Tissue Doppler Imaging and Pulsed Doppler measurements:

Tricuspid and mitral inflows were recorded from an apical 4-chamber view. Tricuspid and mitral inflow early (E) and late (A) velocities were measured from 3 cardiac-cycles and the mean value calculated. As illustrated in **Figures 1A-B**, time to tricuspid valve and mitral valve opening were measured from the onset of the ECG R-wave to the onset of tricuspid and mitral Doppler flow, respectively. Right ventricular (RV) and left ventricular (LV) inflow duration were measured from the Doppler early diastolic (E)-wave onset to late diastolic (A)-wave termination. Pulmonary artery outflow was measured from a short-axis view. Pulmonary and aortic outflow were measured from short-axis and apical 5-chamber views, respectively. We used the conventional definition of the RV and LV isovolumic contraction times (ICT), as incorporating the electro-mechanical delay and isovolumic contraction time as measured from the onset of the ECG Q-wave to onset of pulmonary or aortic Doppler flow, respectively (**Figures 1C-D**). Ejection time (ET) was measured from pulmonary and aortic Doppler flows. LV isovolumic relaxation time (IRT) was measured from termination of aortic flow to onset of the following mitral E-wave using a Doppler sample straddling the LV inflow and outflow (**Figure 1D**). RV IRT was calculated as the time from pulmonary valve closure to tricuspid valve opening (ensuring images had the same HR, **Figure 1C**). For all timing measurements, 3-cardiac cycles were analyzed. We also recorded total cardiac-cycle duration (measured as the ECG, RR-interval) and HR. Tricuspid and mitral lateral annulus pulsed tissue Doppler velocities (systolic velocity (S´), early (E´) and late (A´) diastolic velocities) were obtained from 3-cardiac cycles and the results averaged.

M-mode measurements:

Time to maximum tricuspid and mitral annular systolic excursion (TAPSE, MAPSE) were measured in an apical 4-chamber view from the ECG-R wave onset (**Figure 2**). Time to peak RV and LV free-wall radial thickening were measured from the short-axis (**Figure 3A**). The pattern and sequence of interventricular septal (IVS) motion and time to maximal early-diastolic LV septal bowing were evaluated by M-mode.

2D assessment and interventricular interactions:

The fractional area change (FAC) was calculated as end-diastolic-end-systolic/ end-diastolic RV areas from a 4-chamber view. The LV eccentricity index (EC) was obtained from a short-axis view at the LV papillary muscle level at end-systole, early-diastole and end-diastole (**Figure 4**). Images were analyzed frame-by-frame, simultaneously with the ECG, to describe the IVS configuration and position through the cardiac-cycle.

**Invasively measured hemodynamics:**

At the terminal experiment, hemodynamics were measured immediately after echocardiography using a high-fidelity 2F conductance catheter (Millar Instruments, Houston, Tx) under 3% isoflurane anesthesia. Cardiac output (CO), end-systolic and diastolic volumes and pressures were determined from pressure-volume loops. The maximal rate of ventricular pressure rise and decay (dp/dt max, dp/dt min) were calculated. Tau was assessed as the time constant of mono-exponential decay of ventricular pressure during isovolumic relaxation. Myocardial contractility (elastance, Ees) was determined from a family of pressure-volume loops recorded during transient occlusion of the inferior vena cava. After measuring RV hemodynamics, the catheter was inserted through the LV apex to measure LV hemodynamics.

**Statistical analysis:**

All timing measurements were normalized to the RR-interval and expressed as percentage of the cardiac-cycle. Data are presented as mean±standard deviation. Differences between groups were analyzed with one-way analysis of variance and *post- hoc* least significant difference test (SPSS, IBM). Intra- and inter-observer reliability were evaluated in 20-rats (n=5/ group). A two-way mixed-model (targets conceived as random samples) intraclass correlation coefficient (ICC) for absolute agreement was calculated (5). A $p$-value < 0.05 was considered significant.

**RESULTS:**

Forty rats were studied (15 shams, 8 PAH, 9 PAH+carvedilol, 8 PAH+ivabradine). Their body weight (significantly reduced in all PAH groups as compared to Sham) and echocardiographic timing measurements are summarized in **Table 1** and **Figures 3A-D**. Invasive hemodynamic and functional parameters were obtained from 8 shams, 5 PAH, 9 PAH +carvedilol rats and 7 PAH+ivabradine rats (**Table 2)**.

Heart Rate

HR was reduced by 16% in the PAH+carvedilol and PAH+ivabradine groups vs. shams (302±22 and 304±17 beats per minute vs. 359±31 beats per minute, p<0.001 respectively). PAH rats had statistically similar HR as compared to shams (334±28 vs 359±31 beats per minute, *p=0.295*) (**Table 1**). The results of the LV+S/RV (Fulton) ratio were: control: 0.28±0.03; PAH: 0.68±0.1; PAH+carvedilol: 0.55±0.12; PAH+ivabradine: 0.76±0.1 (all p<0.001 vs. control).

Cardiac-cycle events

In shams, the pulmonary and aortic valves open and close near-simultaneously (**Figure 3A**), while the tricuspid valve opens slightly after the mitral valve. Compared with shams, PAH-rats had significantly increased RV ICT, delayed tricuspid valve opening and reduced RV ET as well

as filling time. PAH-rats also showed increased LV ICT and reduced LV ET as well as filling time (**Figure 3B**). With HR reduction, RV ET and filling time remained short in PAH+carvedilol and PAH+ivabradine (**Figures 3C-D**) (due to high pulmonary vascular resistance, **Table 1**), but timings changed: RV as well as LV ICT shortened significantly, thus shifting timing of valve opening towards normality. Filling time (although only significantly for the LV with carvedilol) had a tendency to normalize.

The delay in RV cardiac-cycle events detailed above in PAH-rats correlated with a significant left-to-right radial motion misalignment between the RV and LV seen on M-mode. RV peak-radial motion occurred significantly later and for a longer duration (**Figure 3B**). Consequently, LV relaxation started while the RV was still contracting. RV and LV longitudinal shortening was largely simultaneous, but significantly delayed in PAH-rats (**Table 1, Figure 3B**) as compared to shams, in which RV and LV peak-radial motion and early-relaxation occurred simultaneously, coinciding with peak-longitudinal TAPSE and MAPSE (**Figure 3A**). Due to prolonged RV systole, reduced RV ejection time in PAH-rats, RV filling time was significantly shortened (**Table 1**) and delayed to late-diastole, coinciding with atrial contraction (**Figure 3B**). As shown in **Table 1**, these findings were also associated with reduced tricuspid and mitral lateral annulus tissue Doppler systolic (S´), early (E´) and late (A´) diastolic velocities. The addition of carvedilol and ivabradine significantly improved LV-RV radial contractile alignment (**Figures 3C-D**), with RV free-wall peak-radial contraction occurring earlier; and as observed on M-mode, faster early RV relaxation (**Figures 3B-D**). Carvedilol also reduced times to peak TAPSE and MAPSE compared with the PAH-group (**Table 1, Figure 3C**) and normalized both tricuspid and mitral lateral annulus systolic and diastolic velocities (**Table 1**). Ivabradine reduced time to peak

TAPSE compared with PAH-group (**Table 1, Figure 3D**) but its effects on tricuspid and mitral annulus systolic and diastolic velocities were more modest (**Table 1**).

Interventricular interactions

Visual analysis of M-mode in shams showed simultaneous IVS, RV and LV lateral free-wall motion, without early-diastolic LV septal bowing (**Figure 3A**). Conversely, 90% of PAH-rats showed early-diastolic leftward septal bowing as a consequence of LV-RV disparate radial motion and delayed RV relaxation described above (**Figure 3B**). Frame-by-frame 2D assessment of IVS configuration in the short-axis view confirmed M-mode findings: shams had a circular LV with normal round IVS curvature and position throughout the cardiac-cycle (**Figure 4A**), while in PAH-rats the RV was markedly enlarged, the LV flattened and 'D-shaped' throughout the cardiac-cycle (**Figure 4B**); with the IVS displaced leftward in systole and early-diastole and flattened into late-diastole. These findings were associated with significantly higher LV EC throughout the cardiac-cycle in PAH-rats vs. controls (**Table 1**). Based on visual M-mode assessment (**Figures 3C-D**) carvedilol and ivabradine led to faster early RV relaxation and significantly reduced time to maximal LV septal bowing compared with untreated PAH-rats (**Table 1, Figures 3B+D**). This corresponded with the shorter tau found in these animals (**Table 2**). Moreover, carvedilol significantly reduced LV EC index in systole and early-diastole (**Table 1**). Although the RV remained enlarged and TV inflow duration short in both treated groups, the improvement in interventricular coupling in early-diastole translated into an increased early diastolic LV filling (E) velocities and normalized lateral mitral annular peak diastolic tissue velocities (**Table 1**). Biventricular early-systolic function was also improved with carvedilol as reflected by reduced time to maximal TAPSE and MAPSE and increased tricuspid and mitral lateral annular peak-systolic tissue velocities (**Table 1**).

Hemodynamics and function:

Hemodynamics and function variables are summarized in **Table 2**. RV peak systolic pressure and RV/LV systolic pressure ratio were increased in all PAH groups vs. shams and not different between PAH groups. The improved RV and LV mechanics, timing and interventricular interactions detailed above with HR reduction corresponded with improved hemodynamics as seen by increased CO, RV contractility (dP/dTmax, Ees) and diastolic relaxation (dP/dTmin, Tau).

Intra-observer and inter-observer reliability:

Intra-observer and inter-observer reproducibility for echo measurements was good (**Table 3**).

**DISCUSSION:**

We evaluated the mechanical effects of HR reduction on cardiac-cycle events and function in experimental PAH. We demonstrate that despite persistent PAH, carvedilol and ivabradine improve early RV relaxation and realign RV-LV radial motion by reducing biventricular ICT and normalizing longitudinal biventricular motion. In particular, these effects improve early LV filling and therefore biventricular systolic and diastolic function and hemodynamics. This detailed analysis provides a mechanistic basis for carvedilol's beneficial effects on biventricular function in PAH and strengthens the basis for investigating its use in clinical PAH (15, 2,3).

Heart-rate effects

Improved interventricular interactions were at least partially, attributable to HR. However, although carvedilol and ivabradine significantly decreased HR in PAH-rats, RV diastolic duration did not lengthen significantly nor did ejection time shorten. Nonetheless, we observed improvements in biventricular diastolic function and ventricular filling. Of note, the mean HR was not different in the PAH-group compared to shams, which differs from the PAH-rats

presented in our previous experiment (15). This difference may be explained by 3 rats not being the same individuals.

Systolic radial alignment

Carvedilol led to re-alignment of RV-LV peak-radial motion. Earlier RV peak-radial motion in the PAH+HR reduction was associated with significant biventricular ICT shortening (**Table 1**). Left-right delay in peak myocardial shortening in PAH patients is caused by prolonged rather than delayed RV contraction (12) including increased ICT. This causes early-diastolic LV septal bowing, decreased LV filling and decreased stroke volume, all important features in the PAH-group. Computer modeling suggests that electrically pre-exciting the RV leads to simultaneous RV-LV contraction thereby improving biventricular function and filling (11). We now show similar beneficial effects on these critical events with carvedilol and ivabradine, despite persistent PAH. Moreover, we demonstrate inefficient RV contraction in PAH as RV peak-radial contraction occurs after pulmonary valve closure, and close to tricuspid valve opening (**Figure 3B**), consistent with RV post-systolic contraction present in PAH patients (12, 13). Overall, HR reduction improved interventricular radial mechanical synchrony due to earlier and shorter ICT and better aligned RV radial mechanics.

Improvements in systolic and diastolic function

RV contractility and relaxation were improved with HR reduction using pressure-volume loop derived end-systolic elastance, time-constant of RV relaxation (tau) and dP/dT minimum (**Table 2**). These are consistent with the improved RV relaxation seen by M-mode and tissue Doppler velocities in the current study, and associated with improved LV filling. Early RV relaxation, as measured by *tau* and decreased diastolic tissue Doppler velocities, is abnormal in clinical PAH even when contractility is still preserved early in the disease course (14, 4). Both impaired

relaxation and post-systolic contraction compromise diastolic function (12, 13). In the present study we demonstrate that carvedilol and ivabradine not only improve RV relaxation and diastolic performance as seen by tissue Doppler imaging, M-mode and Doppler flow, but also enhance biventricular function in early systole. Thus, improved RV relaxation seems important in explaining not only improved RV diastolic, but also systolic function, S:D ratio and early-diastolic interventricular interactions. Together, the re-alignment of radial mechanics and earlier longitudinal motion towards normal induced by HR reduction, lead to improved early-diastolic LV geometry and improved LV filling in early diastole. Peak systolic pressure and cardiac output in the PAH-ivabradine group tended to be higher than the PAH-carvedilol group. The carvedilol treated group may have somewhat lower peak systolic pressures and cardiac output due to a negative inotropic effect versus ivabradine. However, the RV/LV pressure ratio was the same in all groups allowing comparison between them in terms of the PAH.

Postulated mechanisms of action

We did not study the molecular mechanisms underlying the biventricular mechanics investigated in the current study, but these are worthy of a short hypothesis-generating discussion. As ivabradine induced similar effects to carvedilol, the effects could be attributable to a lower HR. However, rather than lengthening RV and LV filling time per se, the effect is based on a change in the timing of events, where ICT shortens and leads to a normalization of the timings in the cardiac cycle that were importantly changed due to the PAH. Related to this, the interventricular interaction changes with HR reduction, thereby attenuating the important septal shift in early diastole. From M-mode images, a restoration of the early outwards motion of the RV wall can be seen, thus also improving early LV filling. While it is difficult to completely distinguish between HR reducing effects versus other components of beta-blocker effects of carvedilol, the similar

improvement in ventricular function and contractility seen in both the carvedilol and ivabradine treated groups suggests that it is HR reduction, rather than beta-blockade per se, that leads to improved function. We postulate that this occurs through re-alignment of RV and LV events and improved diastolic relaxation.

The exact mechanisms remain to be elucidated. One postulated mechanism may relate to the timing of actin-myosin cross-bridging. Increased afterload reduces myocyte shortening velocity and prolongs shortening (25). Thus, RV pressure remains higher for a longer duration than the LV. Consequently, RV actin-myosin cross-bridge cycling may lengthen (hyper-bridging) resulting in stiffer myocardium at end-ejection, prolonging IRT and hampering early-relaxation. Although not proven in this study, HR reduction and associated changes in ICT may improve RV early-relaxation by reducing actin-myosin crossbridging, resulting in more compliant myocardium at end-systole (25, 10). This could explain the observed improvements in RV relaxation, contractility, LV-RV interactions and LV early-diastolic filling, as well as the trend to reduced RV and LV end-diastolic pressures.

We previously showed that carvedilol upregulates RV sarco-endoplasmic-reticulum-$Ca^{2+}$-ATPase2a (SERCA2a) expression in experimental PAH with a similar trend in the LV (15). Downregulated SERCA2a in failing myocardium impairs intracellular calcium cycling, affecting troponin-C binding and actin-myosin crossbridging, worsening contractile and diastolic function (17). Conversely, restoration of SERCA2a improves calcium cycling and cardiac function (17). Based on our current results and prior findings, we hypothesize that HR reduction may improve calcium handling and myocardial relaxation by restoring SERCA2a. This requires confirmation in further studies. Likewise, we previously found biventricular fibrosis in PAH-rats and its amelioration with carvedilol through downregulated transforming-growth-factor-beta signaling

(15). Decreased fibrosis may further explain the observed improvement in systolic and diastolic performance, reduced leftward septal bowing and improved interventricular interactions. Likewise, in our prior study, RV and LV cardiomyocyte diameter were increased with PAH and decreased with carvedilol (reaching statistical significance for the RV), albeit not to baseline size (15). Whether there is a differential effect of pure HR reduction (ivabradine) or additional contractility modulation (carvedilol) remains to be studied.

Possible Clinical implications

Many PAH patients expire from RV failure (9), but cardiac-specific treatments are lacking (6). Beta-adrenergic receptor blockers, and HR reduction in general, improve heart function and survival in left heart failure (16), but are currently contraindicated in PAH because of potential detrimental effects on cardiac output (19). However, we and others have demonstrated in experimental PAH, that beta-adrenergic receptor blockers, and selective inhibition of the sinoatrial inward hyperpolarization-activated current, improve biventricular function, stroke volume, cardiac output and exercise capacity, despite persistent PAH (15, 3, 18). These changes were accompanied by a lower RV S:D ratio (15), a clinically relevant finding as increased S:D ratio is associated with mortality in pediatric PAH (1). Moreover, in early PAH, the RV maintains contractility, but there may be coexisting abnormal early relaxation (14). The results of the current study suggest the need for carefully controlled human trials to test the safety and efficacy of HR reduction in PAH recognizing that the density and distribution of cardiac adrenergic receptors (in the case of beta-blockers) can differ between rodents and humans, which can impact the clinical implications of our findings.

Study limitations

The aim of the present study was to investigate carvedilol's and ivabradine's effects on cardiac-cycle events and mechanics in PAH and we did not evaluate molecular mechanisms. Likewise, we did not directly assess RV compliance or crossbridging. The limitations of experimental PAH models are well known. Relevant to the current study, we previously demonstrated in a monocrotaline-PAH that carvedilol did not act through alleviation of myocarditis or lung inflammation, both absent in these animals (15). Importantly, PAH was persistent, allowing study of carvedilol's and ivabradine's biventricular effects without the confounding effect of decreased pulmonary vascular resistance. The 12-mHz probe used in this study is of relatively low frequency. However, we have found that in rats the 12-Mhz transducer often produces better quality images than very high frequency transducers designed predominantly for use in mice and have recently reported good feasibility and reproducibility using a 10 Mhz probe in a rabbit model (20). In the current study, we also performed inter and intra-observer reliability which was found to be good (Table 3). Moreover, the same probe was used across all groups and thus the comparison is subject to the same conditions and is valid.

Conclusion

In conclusion, we demonstrate that in experimental PAH, HR reduction improves RV early-relaxation and diastolic function, leading to re-alignment of systolic RV-LV peak-radial mechanics and interventricular interactions. These improved mechanics and biventricular function were associated with improved cardiac output and hemodynamics.

**Disclosures**

None

## BIBLIOGRAPHY


1-Alkon J, Humpl T, Manlhiot C et al. (2010) Usefulness of right ventricular systolic to diastolic duration ratio to predict functional capacity and survival in children with pulmonary arterial hypertension. Am J Cardiolog 3:430-436.

2-Bogaard HJ, Abe K, Vonk-Noordegraaf A et al (2009). The right ventricle under pressure: Cellular and molecular mechanisms of right heart failure in pulmonary hypertension. Chest;135:794–804.

3-Bogaard HJ, Natarajan R, Mizuno S at al. (2010) Adrenergic receptor blockade right heart remodeling and dysfunction in pulmonary hypertensive rats. Am J Res Crit Car Med 182:652-660.

4-Faludi R, Komócsi A, Bozó J et al. (2008) Isolated diastolic dysfunction of right ventricle: stress-induced pulmonary hypertension. Eur Respir J ;31(2):475–476.

5-Fleiss J. Statistical Methods for Rates and Proportions. In John Wiley and Sons: New York (2nd edition). 1981

6-Galie N, Hoeper MM, Humbert M et al. The Task Force for the Diagnosis and Treatment of Pulmonary Hypertension of the European Society of Cardiology (ESC) and the European Respiratory Society (ERS) endorsed by the International Society of Heart and Lung Transplantation (ISHLT). (2009) Guidelines for the diagnosis and treatment of pulmonary hypertension. Eur Respir J;34:1219–1263.

7-Gan CT, Lankhaar JW, Marcus JT et al. (2006) Impaired left ventricular filling due to right-to-left ventricular interactions in patients with pulmonary arterial hypertension. Am J Physiol Heart Circ Physiol 290:1528-1533.

8-Hardegree EL, Schadev A, Fentad ER et al. (2013) Impaired left ventricular mechanics in pulmonary arterial hypertension. Cir Heart Fail ; 6: 748-755.

9-Humbert M, Sitbon O, Simonneau G. (2004) Treatment of pulmonary arterial hypertension. N Engl J Med 2004;351:1425–1436.

10-Lee JA, Allen DG. (1997) Calcium sensitizers: mechanisms of action and potential usefulness as inotropes. Cardiovascular research;36:10-20.

11-Lumens J, Arts T, Broers B et al. (2009) Right ventricular free wall pacing improves cardiac pump function in severe pulmonary arterial hypertension: a computer simulation analysis. Am J Physiol Heart Circ Physiol:297(6): H2196-H2205.

12-Marcus JT, Gan TJ Zwanenburg J et al. (2008) Interventricular mechanical asynchrony in pulmonary arterial hypertension. Left-to-right delay in peak shortening related to right ventricular overload and left ventricular underfilling. J Am Coll Cardiol;51:750-757.

13-Mauritz G-J, Marcus JT, Westerhof N et al. (2011) Prolonged right ventricular post-systolic isovolumic period in pulmonary arterial hypertension is not a reflection of diastolic dysfunction. Heart; 97(6):473–478.

14-Murch SD, La Gerche A, Roberts T et al. (2015) Abnormal right ventricular relaxation in pulmonary hypertension. Pulmonary Circulation; 5 (2):370-375.

15-Okumura K, Kato H, Honjo O et al. (2015) Carvedilol improves biventricular fibrosis and function in experimental pulmonary hypertension. J Mol Med ,93:663-74.

16-Packer M, Coats AJS, Fowler MB et al. (2001) Effect of carvedilol on survival in severe chronic heart failure. N Engl J Med 2001;344:1651–1658.

17-Periasamy M, Bhupathy P, Baby GJ. (2008) Regulation of sarcoplasmic reticulum ca2+ ATPase pump expression and its relevance to cardiac muscle physiology and pathology. Cardiovasc Res 2008;77:265-273.

18-Perros F, Ranchoux B, Izikki M et al. (2015) Nebivolol for Improving Endothelial Dysfunction, Pulmonary Vascular Remodeling, and Right Heart Function in Pulmonary Hypertension. J Am Coll Cardiol;65:668–680.

19-Provencher S, Herve P, Jais X et al. (2006) Deleterious effects of Beta-adrenergic receptor blockers on exercise capacity and hemodynamics in patients with portopulmonary hypertension. Gastroenterology;130:120–126.

20- Ramos SR, Pieles G, Hui W et al (2017) Comprehensive echocardiographic assessment of biventricular function in the rabbit, animal model in cardiovascular research: feasibility and normal values. Int J Cardiovasc Imaging; in press (doi: 10.1007/s10554-017-1238-4).

21-Sarnari R, Kamal RY, Friedberg MK et al. (2009) Doppler assessment of the systolic to diastolic duration in normal children: relation to heart rate, age and body surface area. J Am Soc Echocardiography; 22:928-932.

22-Simon L, Ghaleh B, Puybasset L, et al. (1995) Coronary and hemodynamic effects of s 16257, a new bradycardic agent, in resting and exercising conscious dogs. J Pharmacol Exp Ther; 275:659-666.

443 23-Thollon C, Cambarrat C, Vian J, et al. (1994) Electrophysiological effects of s
444 16257, a novel sino-atrial node modulator, on rabbit and guinea-pig cardiac preparations:
445 Comparison with ul-fs 49 . Br J Pharmacol;112:37-4.

446 24-Thollon C, Bidouard JP, Cambarrat C, et al . (1997) Stereospecific in vitro and in vivo
447 effects of the new sinus node inhibitor (+)-s 16257. Eur J Pharmacol ; 339:43-51.

448 25-Tombe P, Keurs H. (2012) The velocity of cardiac sarcomere shortening: mechanisms and
449 implications. Muscle Res Cell Motil ;33(6):431–437.
450
451
452
453

454 **TABLES**

| | Sham (n=15) | PAH (n=8) | PAH +carvedilol (n=9) | PAH+ ivabradine (n=8) |
|---|---|---|---|---|
| Body weight (gr) | 472.6±48.6 | 397.1±53.3$^{*}$ | 403.6±73.8$^{*}$ | 349.2±22.1$^{**}$ |
| HR (bpm) | 359± 31.2$^{§§§,µµµ}$ | 334± 27.6 | 302.5 ± 21.8$^{***}$ | 303.6± 17.1$^{***}$ |
| RR- interval (ms) | 167.6 ± 14.9$^{§§§,µµµ}$ | 180.1± 15.2 | 198.5± 14.5$^{***}$ | 198.5± 12.2$^{***}$ |
| **Functional parameters** | | | | |
| TV E (cm/s) | 0.50 ± 0.1 | 0.69 ± 0.1 | 0.57 ± 0.3 | 0.54 ± 0.1 |
| TV A (cm/s) | 0.70 ± 0.1 | 0.55 ± 0.1 | 0.69 ± 0.3 | 0.54 ± 0.2 |
| RV *E´*(cm/s) | 6.4 ± 2.1$^{ŧŧ,µ}$ | 3.7 ± 1.3$^{**,§}$ | 6.0 ± 1.2$^{ŧ}$ | 4.25± 0.7$^{*}$ |
| RV *A´*(cm/s) | 6.1 ± 1.8$^{ŧ}$ | 4.0 ± 1.5$^{*}$ | 5.0 ± 1.4 | 4.1 ± 1.5 |
| RV *S´*(cm/s) | 6.3 ± 1.3$^{ŧŧŧ}$ | 3.5 ± 0.6$^{***,§§,µµ}$ | 6.1 ± 1.5$^{ŧŧ}$ | 5.9 ± 1.1$^{ŧŧ}$ |
| RV FAC (%) | 43.0± 5.0$^{ŧŧŧ,§}$ | 24.5 ± 7.1$^{***,µµ}$ | 33.8 ± 7.6$^{*}$ | 36.1 ± 7.3$^{ŧŧ}$ |
| MV E (cm/s) | 0.81 ± 0.1$^{ŧŧ}$ | 0.56 ± 0.1$^{**}$ | 0.71 ± 0.2 | 0.67± 0.1 |
| MV A (cm/s) | 0.74 ± 0.1 | 0.65 ± 0.1 | 0.64 ± 0.2 | 0.58± 0.1 |
| LV *E´*(cm/s) | 5.3 ± 1.1$^{ŧŧ}$ | 3.4 ± 1.1$^{**,§§,µ}$ | 5.3 ± 1.1$^{ŧ}$ | 4.9± 0.1$^{ŧ}$ |
| LV *A´*(cm/s) | 6.2 ± 0.4$^{ŧ,µ}$ | 4.5 ± 2.0$^{*}$ | 4.7 ± 1.8 | 4.4 ± 0.9$^{*}$ |
| LV *S´*(cm/s) | 6.8 ± 1.3$^{ŧ}$ | 4.6 ± 2.0$^{*}$ | 5.9 ± 1.7 | 6.25± 1.5 |
| **Left ventricle eccentricity index** | | | | |
| End-systolic EC | 1.2 ± 0.1$^{ŧŧŧ,µµ}$ | 2.0 ± 0.4$^{***,§§}$ | 1.4 ± 0.3$^{ŧŧ}$ | 1.70 ± 0.3$^{**}$ |
| Early-diastolic EC | 1.1 ± 0.1$^{ŧŧŧ,µµµ}$ | 2.1 ± 0.5$^{***,§§}$ | 1.5 ± 0.4$^{ŧŧ}$ | 1.9 ± 0.4$^{***}$ |
| End-diastolic EC | 1.1± 0.1$^{ŧŧŧ,§,µµµ}$ | 1.6 ± 0.3$^{***}$ | 1.4 ± 0.3$^{*}$ | 1.6 ± 0.3$^{***}$ |
| **Pulsed Doppler timing parameters** | | | | |
| RV ICT | 15.2 ± 3.7$^{ŧŧ}$ | 21.8 ± 3.3$^{**,§,µ}$ | 15.6 ± 6.4$^{ŧ}$ | 15.9 ± 1.7$^{ŧ}$ |
| RV ET | 44.0 ± 4.0$^{ŧŧ,§§,µµ}$ | 35.7 ± 3.6$^{**}$ | 35.4 ± 9.2$^{**}$ | 35.9 ± 2.0$^{**}$ |
| Time-to-PVC | 59.2 ± 6.5$^{§}$ | 57.3 ± 3.6 | 48.4± 13.4$^{*}$ | 51.75± 3.21 |
| Time-to-TVO | 70.3 ± 6.4 | 77.7 ± 8.9$^{§,µµ}$ | 66.5 ± 8.6$^{ŧ}$ | 64.5± 4.0$^{ŧŧ}$ |
| RV inflow duration | 41.2 ± 5.5$^{ŧŧŧ,§§,µ}$ | 26.8 ± 3.4$^{***}$ | 30.1 ± 7.2$^{**}$ | 32.1 ± 7.3$^{**}$ |
| RV IRT | 10.6 ± 4.5 | 23.1 ± 15.5 | 18.9 ± 17.5 | 14.1± 2.7 |
| LV ICT | 15.8± 4.2$^{ŧŧŧ}$ | 23.6 ± 4.9$^{***,§§§,µ}$ | 14.0 ± 3.0$^{ŧŧŧ}$ | 17.5 ± 2.6$^{ŧŧ}$ |
| LV ET | 42.1 ± 4.1$^{ŧŧŧ,§§§,µµµ}$ | 30.7 ± 3.7$^{***}$ | 31.0 ± 3.4$^{***}$ | 31.0 ± 3.0$^{***}$ |
| Time-to-AVC | 57.9 ± 6.9$^{§§§,µµ}$ | 54.4 ± 4.3$^{§§}$ | 45.0 ± 4.2$^{***,ŧŧ}$ | 48.4± 1.9$^{**}$ |
| Time-to-MVO | 68.6 ± 6.2$^{§§}$ | 70.7 ± 3.9$^{§§,µ}$ | 60.5 ± 6.1$^{**,ŧŧ}$ | 63.0 ± 4.2$^{ŧ}$ |
| LV inflow duration | 39.3 ± 2.9$^{ŧ}$ | 33.3 ± 4.8$^{*,§}$ | 39.3 ± 5.6$^{ŧ}$ | 37.7 ± 5.0 |
| LV IRT | 12.9 ± 2.4 | 15.5 ± 3.1 | 14.9 ± 2.4 | 13.8 ± 2.3 |
| **M-mode timing parameters** | | | | |
| Time-to-RV peak-radial motion | 58.0 ± 5.1$^{ŧŧŧ}$ | 71.3 ± 10.0$^{***,§§§,µµ}$ | 54.6 ± 6.8$^{ŧŧŧ}$ | 58.6 ± 8.6$^{ŧŧ}$ |
| Time- to- LV peak- radial motion | 58.5 ± 5.8$^{§§,µµ}$ | 54.9 ± 5.5 | 46.3 ± 11.2$^{**}$ | 48.6 ± 7.5$^{**}$ |
| Time-to- maximum LVSB | ---- | 75.5 ± 9.6$^{§,µ}$ | 59.7 ± 9.5$^{ŧ}$ | 63.2 ± 9.2$^{ŧ}$ |
| Time-to-maximum TAPSE | 57.3 ± 6.8$^{ŧŧ}$ | 69.2 ± 6.6$^{**,§§§,µµ}$ | 50.3 ± 8.8$^{ŧŧŧ}$ | 57.0 ± 5.7$^{ŧŧŧ}$ |

| | | | | |
|---|---|---|---|---|
| Time-to-maximum MAPSE | 56.0 ± 8.1$^{t}$ | 66.9 ± 3.6$^{**,§§}$ | 51.3 ± 10.5$^{tt}$ | 56.3± 8.1 |

**Table 1. Summary of echo measurements.** Data shown as mean ± SD. Timing measurements are normalized to their RR-interval and are expressed as percentages. PAH= pulmonary hypertension, HR= heart rate, bpm= beats per minute, ms= milliseconds. **Functional echocardiographic parameters**: TV=tricuspid valve, MV= mitral valve, LV= left ventricle, RV= right ventricle, FAC= Fractional area change. **Doppler timing:** ICT= isovolumic contraction time, ET=ejection time, PVC= pulmonary valve closure, TVO= tricuspid valve opening, AVC= aortic valve closure, MVO= mitral valve opening, IRT= isovolumic relaxation time. **M-mode timing**: IVS= interventricular septum, LVSB= early-diastolic LV septal bowing, TAPSE= tricuspid systolic annular excursion, MAPSE= mitral systolic annular excursion.

*p<0.05, **p<0.01, ***p<0.001 vs sham rats.

$^{t}$p<0.05, $^{tt}$p<0.01, $^{ttt}$p<0.001 vs PAH rats.

$^{§}$p<0.05, $^{§§}$p<0.01, $^{§§§}$p<0.001 vs PAH-carvedilol rats.

$^{µ}$p<0.05, $^{µµ}$p<0.01, $^{µµµ}$p<0.001 vs PAH-ivabradine rats.

| | Sham (n=8) | PAH (n=5) | PAH +carvedilol (n=9) | PAH + ivabradine (n=7) |
|---|---|---|---|---|
| CO (mL/min) | 103.6 ± 60.5 | 34.9 ± 22.3 | 57.9 ± 33.8 | 79.8 ± 27.4 |
| **Right ventricle parameters** | | | | |
| Peak Systolic pressure (mmHg) | $23.4 \pm 1.9^{t,\S\S,\mu\mu\mu}$ | $58.1 \pm 21.6^{*}$ | $55.4 \pm 24.5^{**}$ | $68.1 \pm 14.9^{***}$ |
| End-diastolic pressure (mmHg) | 1.7 ± 1.2 | 3.7 ± 2.9 | 1.43± 1.3 | 2.5 ± 1.6 |
| dP/dt max (mmHg/sec) | $1011.7 \pm 397.6^{\S\S,\mu\mu\mu}$ | 1739.7 ± 457 | $1980.2 \pm 696.7^{**}$ | $2313.8\pm 430.9^{***}$ |
| dP/dt min (mmHg/sec) | $-740.0 \pm 166.1^{\S,\mu}$ | -1720.5± 671 | $-1827.9 \pm 1006.9^{*}$ | $-2063.3 \pm 840.8^{*}$ |
| Ees (mmHg/mL) | 121.4 ± 90.2 | 26.9 ± 11.2 | 114.7 ± 69.8 | 191.4 ± 70.3 |
| Tau (ms) | $7.00 \pm 1.4^{tt}$ | $13.2\pm 2.4^{*,\mu}$ | 10.11 ± 2.9 | $8.6 \pm 2.2^{t}$ |
| **Left ventricle parameters** | | | | |
| Peak Systolic pressure (mmHg) | 78.1 ± 14.1 | 65.4 ± 17.9 | 66.1 ± 22.7 | 76.0 ± 26.7 |
| End-diastolic pressure (mmHg) | 3.9± 0.7 | 3.4± 3.0 | 2.5± 1.5 | 4.0± 1.2 |
| dP/dt max (mmHg/sec) | 3195.2 ± 618.2 | 2768.3 ± 1212 | 3048.9 ± 1389.0 | 3236.4 ± 1133.1 |
| dP/dt min (mmHg/sec) | -2650.4 ± 649.6 | -1537.2 ± 822 | -1989.3± 1035.9 | -1804.8± 706.0 |
| Ees (mmHg/mL) | 289.7 ± 344.0 | 53.8 ± 11.0 | 330.7 ± 284.6 | 157.3 ± 93.2 |
| Tau (ms) | 8.6 ± 1.5 | 9.3 ± 4.9 | 9.3 ± 3.9 | 8.0± 2.4 |
| RVp/LVp | $0.3\pm 0.1^{t,\S\S,\mu\mu}$ | $0.9 \pm 0.3^{*}$ | $0.9\pm 0.3^{**}$ | $0.9 \pm 0.2^{**}$ |

**Table 2. Summary of invasive hemodynamic and functional parameters.** Data shown as mean ± SD. PAH= pulmonary hypertension, CO= cardiac output, Ees= end-systolic elastance.

*p<0.05, **p<0.01, ***p<0.001 vs sham rats.

$^{t}$p<0.05, $^{tt}$p<0.01, $^{ttt}$p<0.001 vs PAH rats.

$^{\S}$p<0.05, $^{\S\S}$p<0.01, $^{\S\S\S}$p<0.001 vs PAH-carvedilol rats.

$^{\mu}$p<0.05, $^{\mu\mu}$p<0.01, $^{\mu\mu\mu}$p<0.001 vs PAH-ivabradine rats.

| Echocardiographic parameter | Intra-observer ICC | 95%-CI | *p** | Inter-observer ICC | 95%-CI | *p** |
|---|---|---|---|---|---|---|
| t-MVO | 0.95 | (0.81-0.98) | *0.000* | 0.92 | (0.57-0.98) | *0.000* |
| RV ICT | 0.78 | (0.24-0.94) | *0.011* | 0.96 | (0.88-0.99) | *0.000* |
| t-LV peak-radial motion | 0.86 | (0.54-0.96) | *0.001* | 0.82 | (0.44-0.94) | *0.002* |
| t-maximum TAPSE | 0.76 | (0.14-0.93) | *0.016* | 0.92 | (0.76-0.97) | *0.000* |
| LV End-systolic EC | 0.78 | (0.34-0.93) | *0.003* | 0.63 | (-0.03-0.87) | *0.024* |

**Table 3. Intra-observer and inter-observer variability.** ICC= intraclass correlation coefficient; 95%-CI= 95% confidence interval; RV= right ventricle, LV= left ventricle, t-MVO=time-to-mitral valve opening; ICT= isovolumic contraction time; t-LV=time-to-LV peak-radial motion; t-TAPSE=time-to-maximum tricuspid systolic annular excursion; EC=eccentricity index. $p^* < 0.05$ considered significant.

## FIGURES TITTLES AND LEGENDS

**Figure 1: Panel A:** Timing measurements of tricuspid valve inflow. Time to tricuspid valve opening (measurement **a**) was measured from the onset of the ECG R-wave to the onset of tricuspid flow. Right ventricle inflow duration (measurement **b**) was measured from the early diastolic (E)-wave onset to late diastolic (A)-wave termination. Time from closure-to opening of the tricuspid valve (measurement **c**) was calculated from late diastolic (A)-wave termination to the next early diastolic (E) wave onset. **Panel B:** Timing measurements of mitral valve inflow. Time to mitral valve opening (measurement **a**) was measured from the onset of the ECG R-wave to the onset of mitral flow. Left ventricle inflow duration (measurement **b**) was measured from the early diastolic (E)-wave onset to late diastolic (A)-wave termination. **Panel C:** Pulmonary outflow from a short axis right ventricle outflow view. Right ventricle isovolumic contraction time (measurement **d**) was measured from the onset of ECG R-wave to the onset of the pulmonary flow. Ejection time (measurement **e**) was measured from pulmonary flow (* pulmonary valve closure). Right ventricular isovolumic relaxation time was calculated from closure-to opening of the tricuspid valve (measurement **c** from panel A; including the isovolumic contraction + the ejection + the isovolumic relaxation times) and then subtracting the isovolumic contraction (measurement **d**) +the ejection time (measurement **e**) from that interval. **Panel D**: Simultaneous sampling of aortic outflow and mitral inflow from an apical 5-chamber view. Left ventricle isovolumic contraction time (measurement **d**) was measured from the onset of ECG R-wave to the onset of the aortic flow. Ejection time (measurement **e**) was measured from aortic flow (* aortic valve closure). Left ventricular isovolumic relaxation time (measurement **f**) was measured from termination of the aortic flow to the onset of mitral early diastolic flow (E-wave). The total cardiac cycle was defined as the ECG RR interval.

**Figure 2:** t= time from the onset of the ECG R-wave (dotted line) to the maximum tricuspid annular systolic excursion (TAPSE) and mitral annular systolic excursion (MAPSE) by M-mode,

in an apical 4-chamber from a rat with pulmonary arterial hypertension. The total cardiac cycle was defined as the ECG RR interval.

**Figure 3:** Left: M-mode echocardiography depicting left (LV) and right ventricular (RV) free-wall radial motion in **panel A)** sham, **panel B)** PAH, **panel C)** PAH+carvedilol and **panel D)** PAH+ivabradine. PAH= pulmonary hypertension. (**) Marks the bowing of the interventricular septum (IVS) towards the left in LV early-diastole (LVSB). Mean RR-interval by group is shown. Right: Schematic representation of the summary of timing measurements: **panel A)** sham, **panel B)** PAH, **panel C)** PAH+carvedilol and **panel D)** PAH+ivabradine. **Doppler timing**: PVO= pulmonary valve opening, AVO= aortic valve opening, PVC= pulmonary valve closure, AVC= aortic valve closure, TVO= tricuspid valve opening, MVO= mitral valve opening. **M-mode timing**: RV= RV peak-radial motion, LV= LV peak-radial motion, tTAPSE= maximum tricuspid systolic annular excursion, tMAPSE= maximum mitral systolic annular excursion.

**Figure 4:** Short-axis view at left ventricular (LV) papillary muscles level in **panel A)** sham, **panel B)** PAH , **panel C)** PAH+carvedilol and **panel D)** PAH+ivabradine. PAH= pulmonary arterial hypertension. RV= right ventricle. The position of the interventricular septum (**) throughout cardiac-cycle is shown.

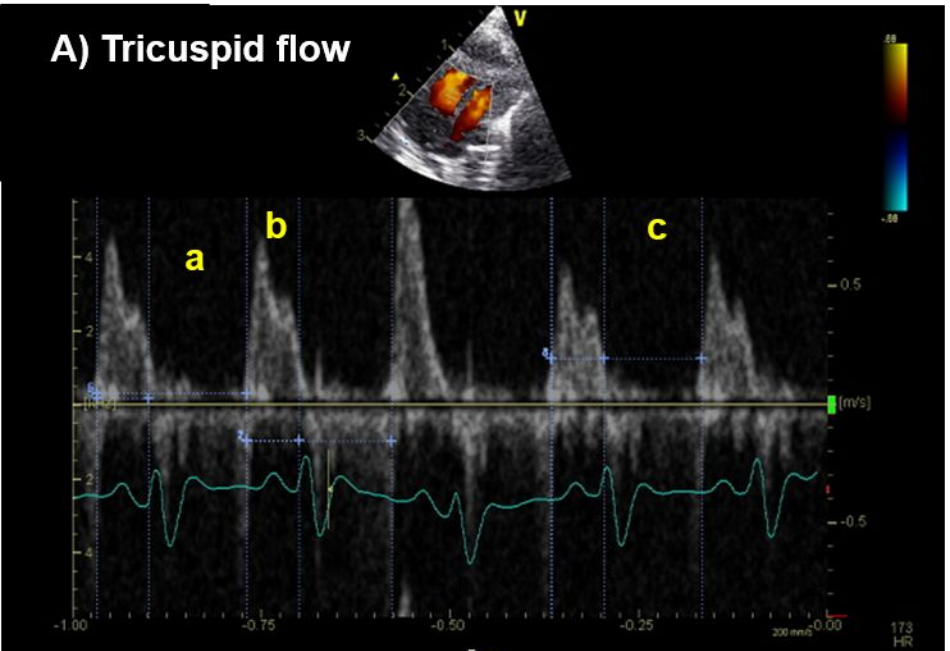
A) Tricuspid flow
a
b
c
(m/s)
173
HR

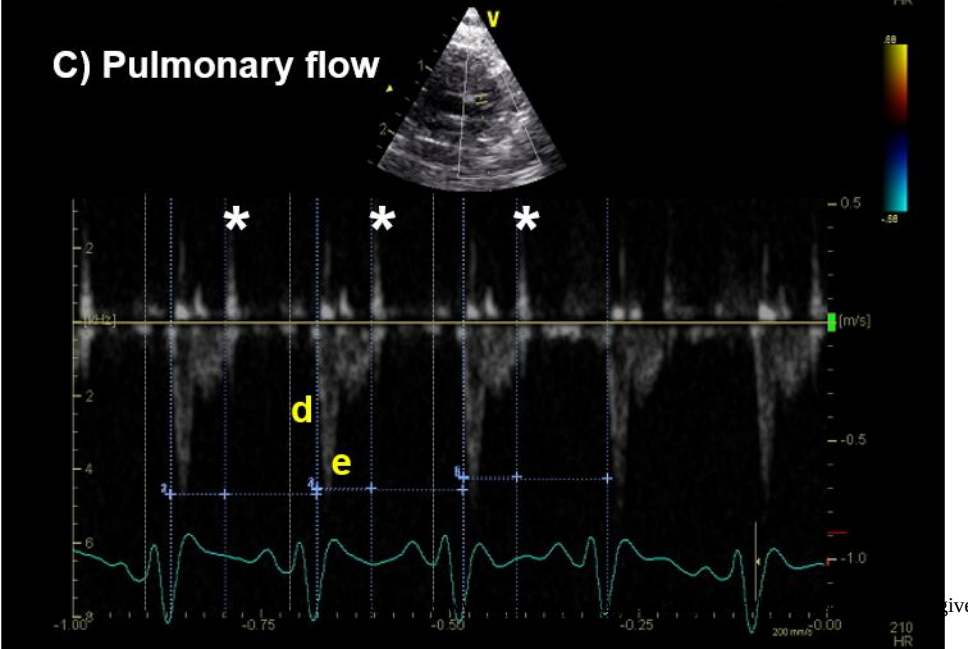
C) Pulmonary flow
*
*
*
d
e
(m/s)
210
HR

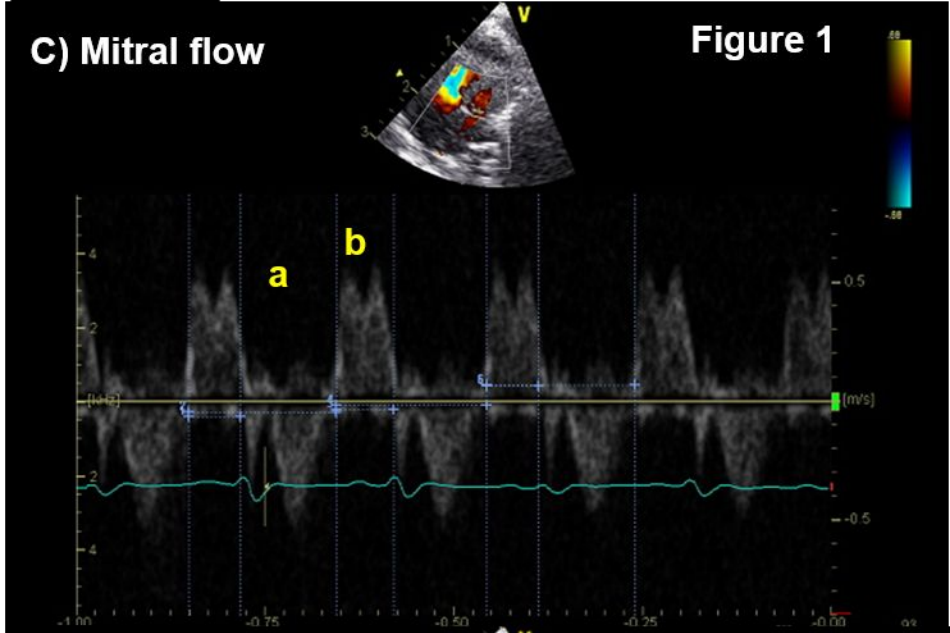
C) Mitral flow
a
b
(m/s)

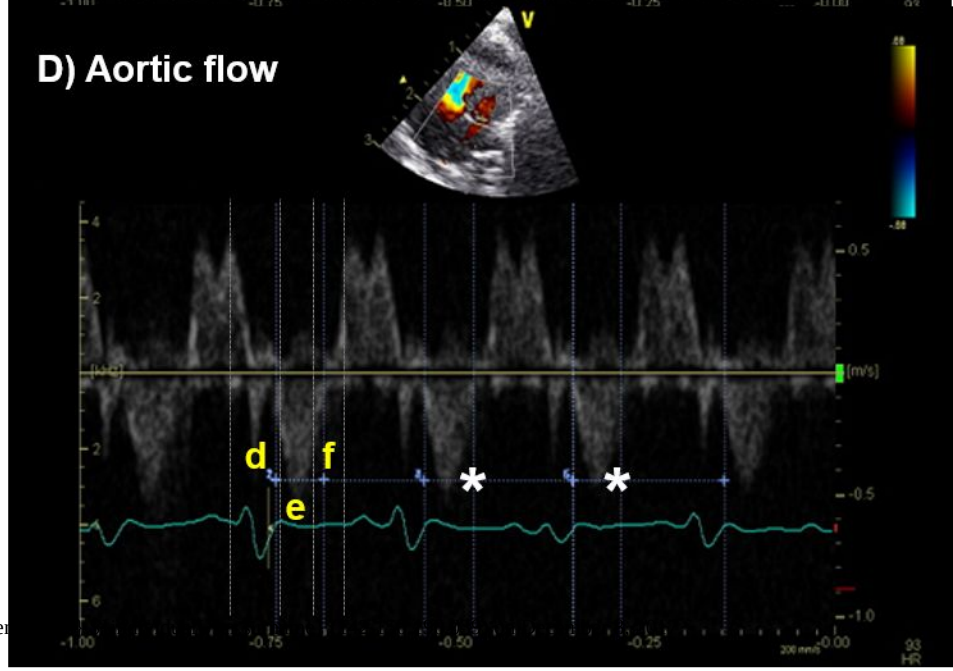
D) Aortic flow
d
e
f
*
*
(m/s)
93
HR

Figure 1

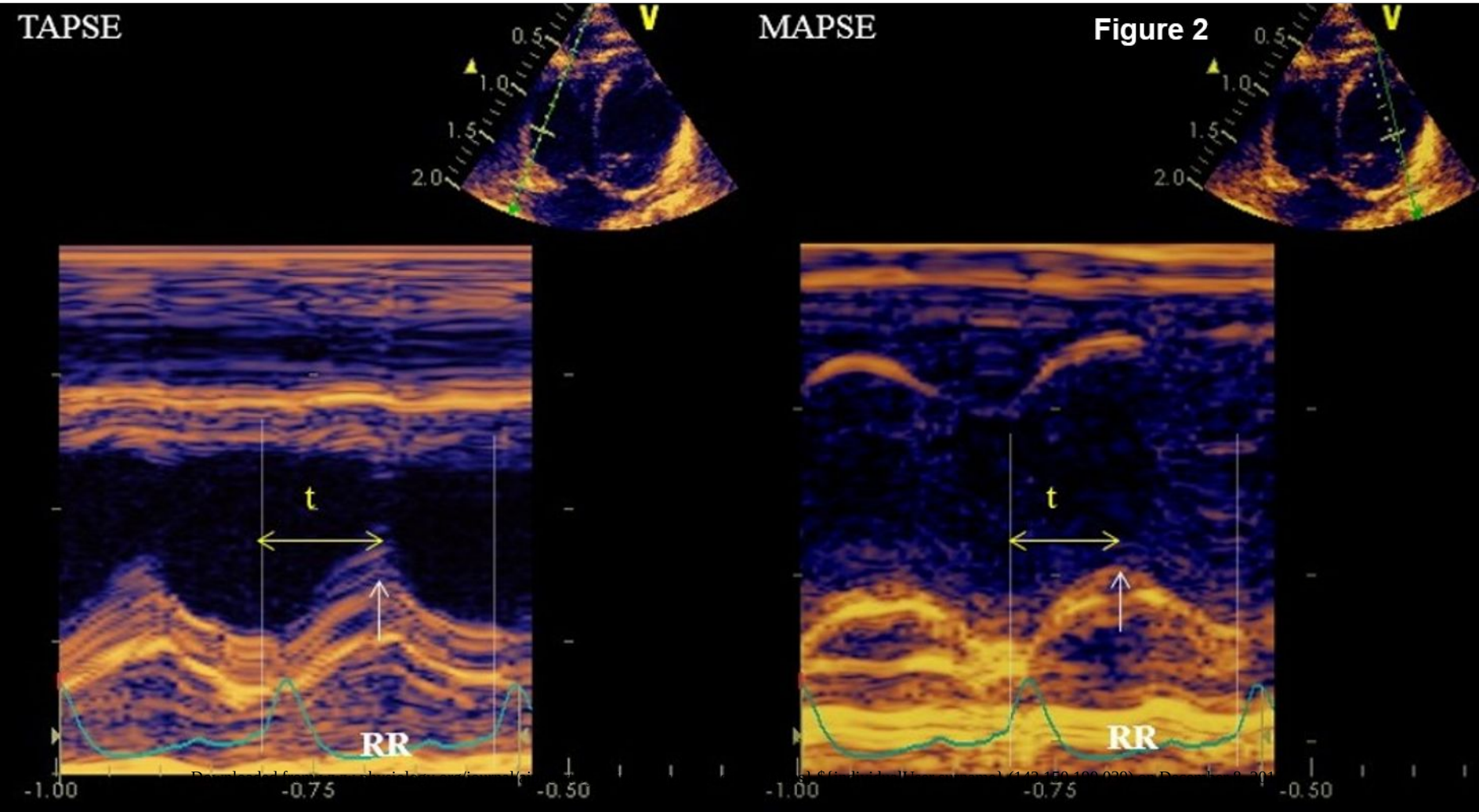
TAPSE
MAPSE
Figure 2
t
RR
t
RR
-1.00
-0.75
-0.50
-1.00
-0.75
-0.50

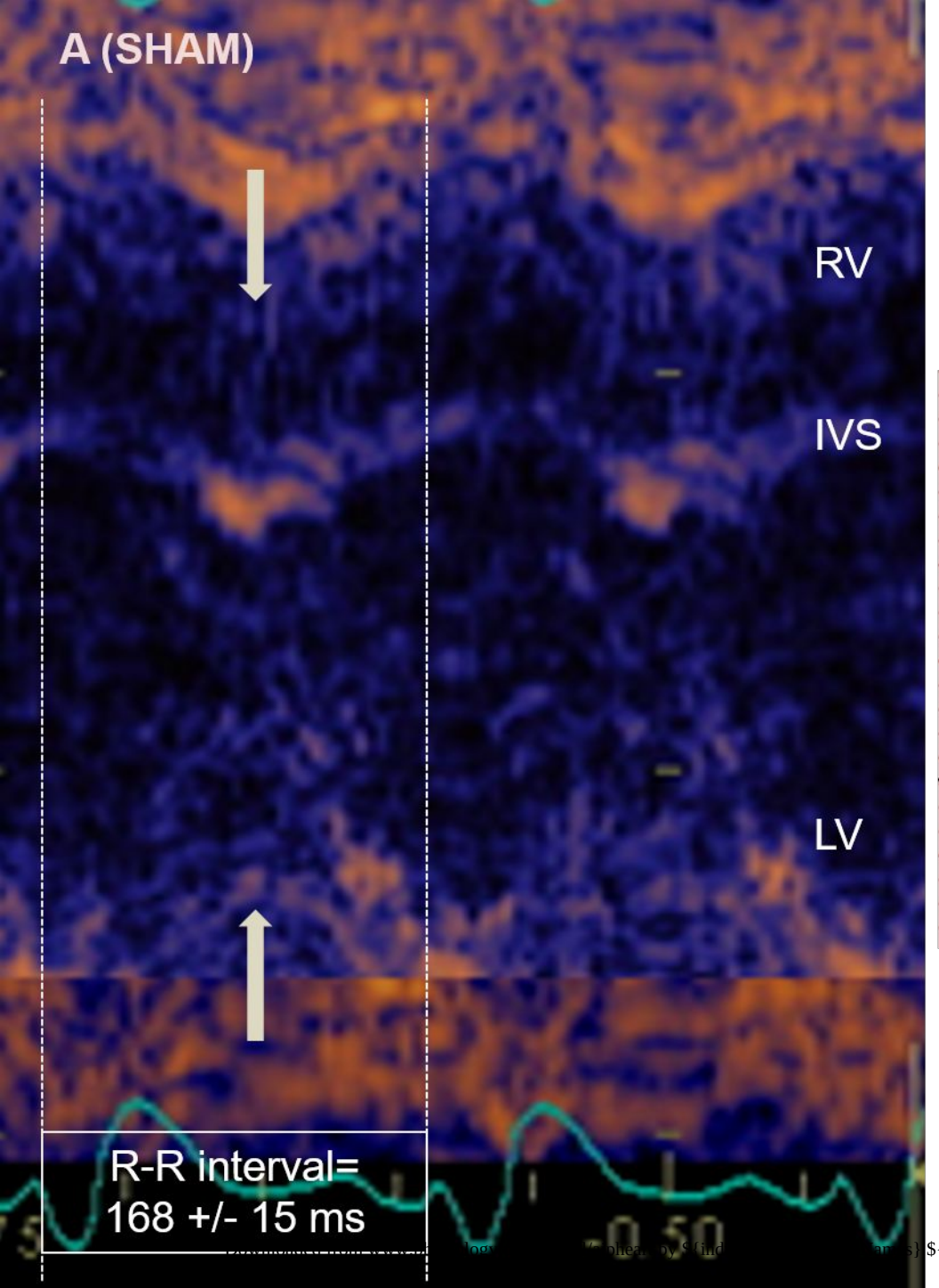


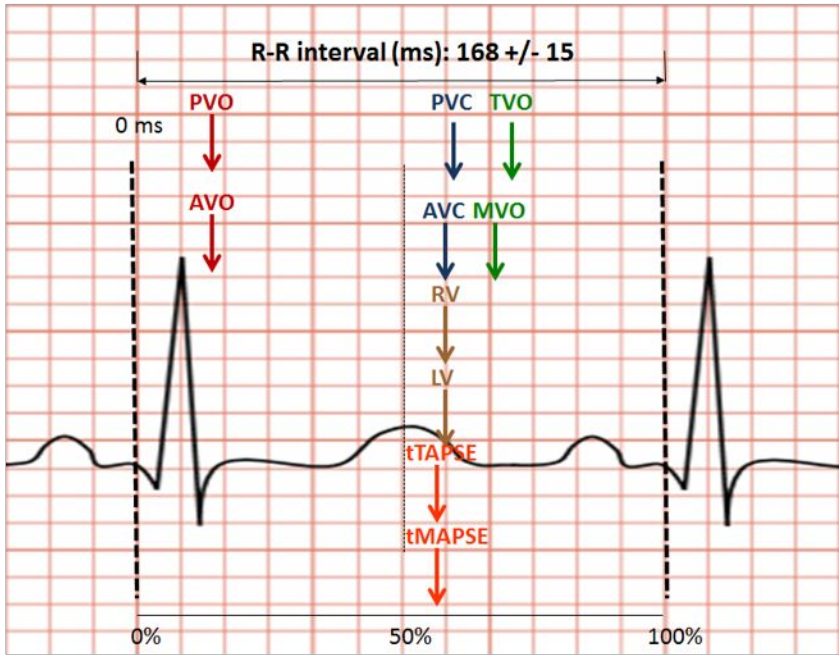

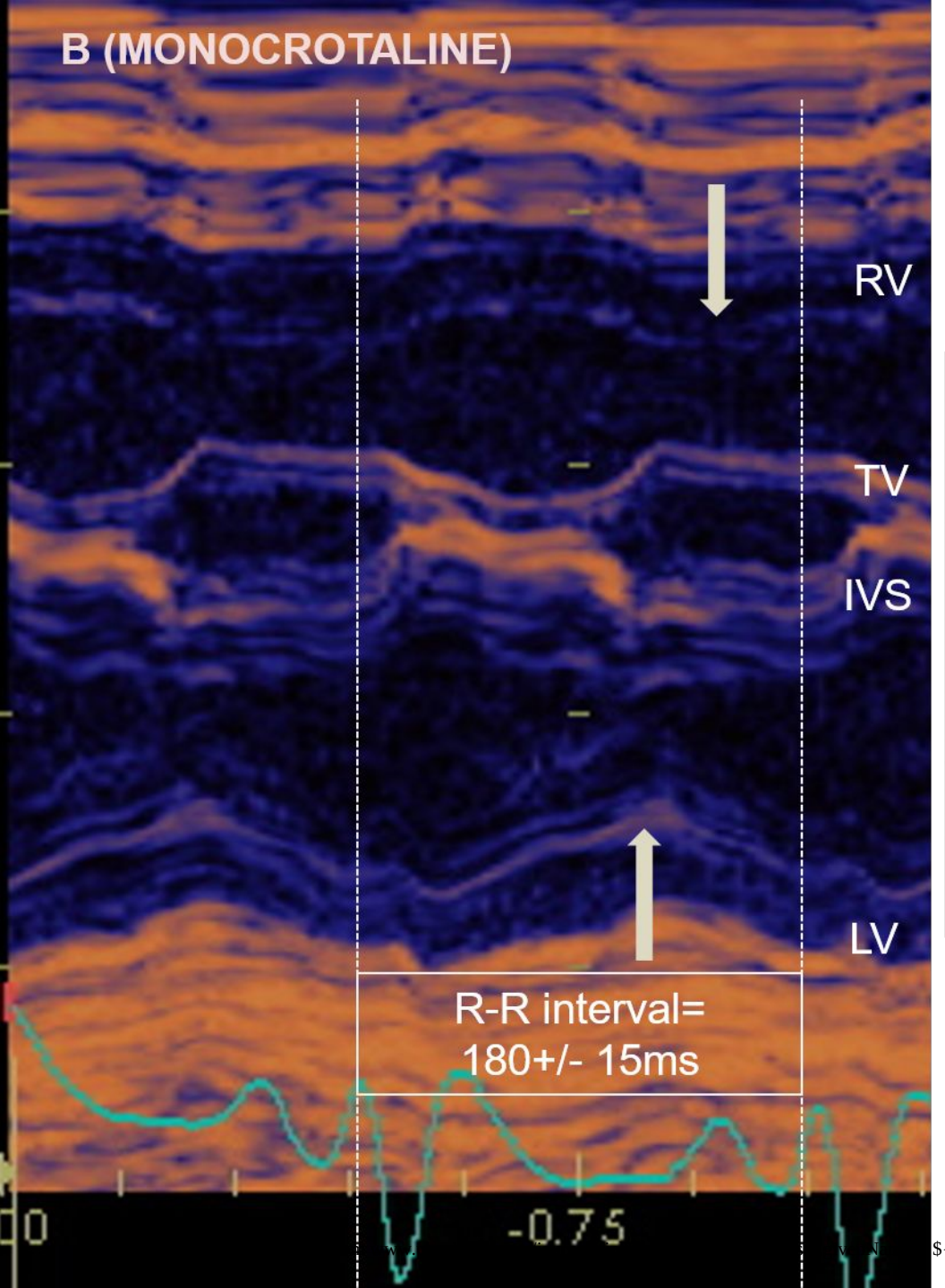


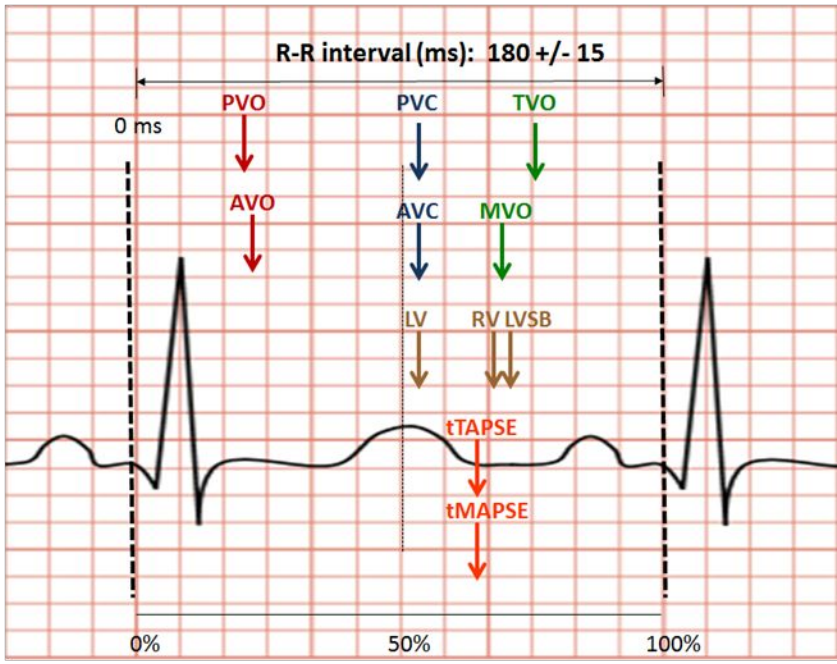

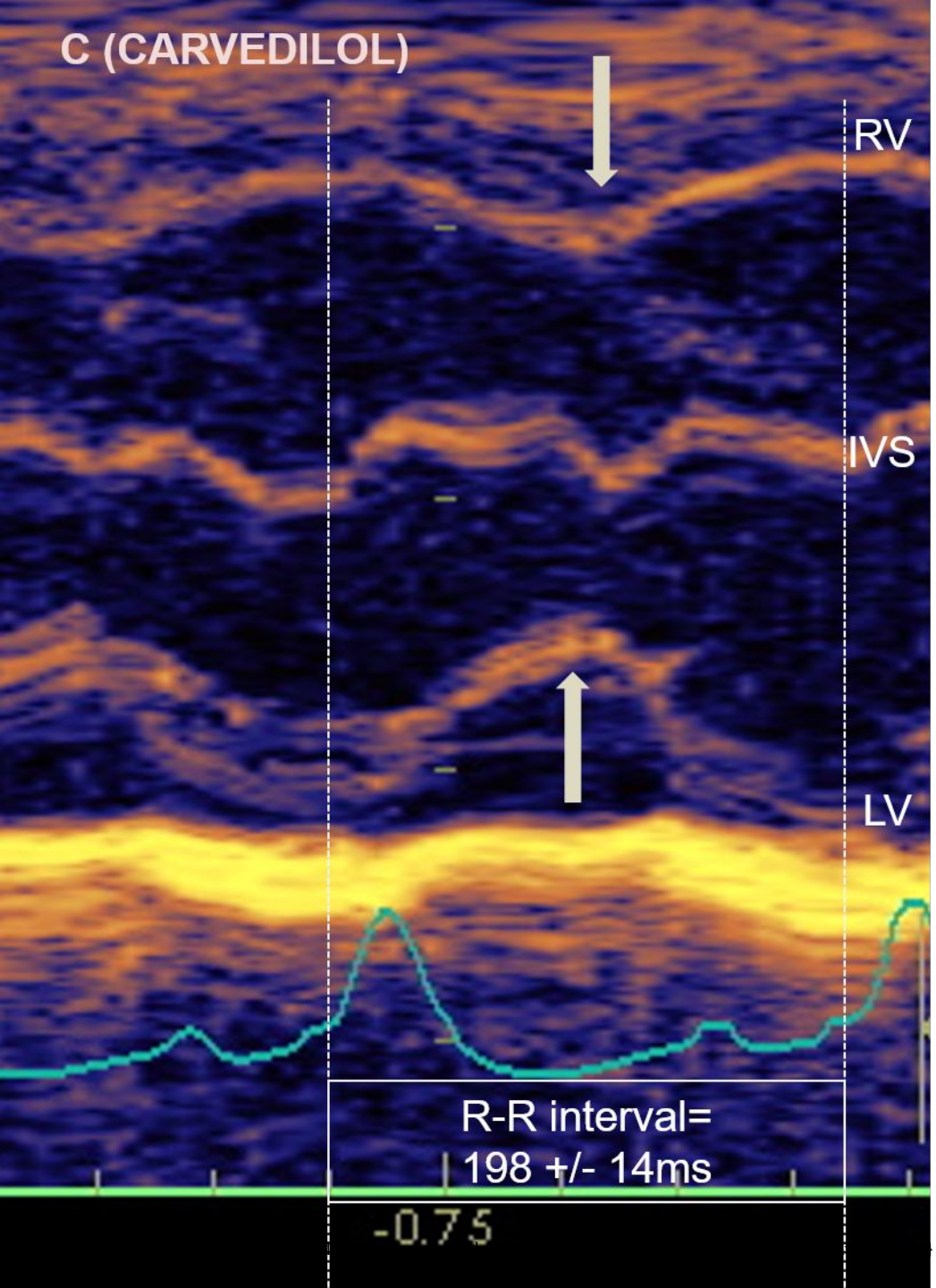


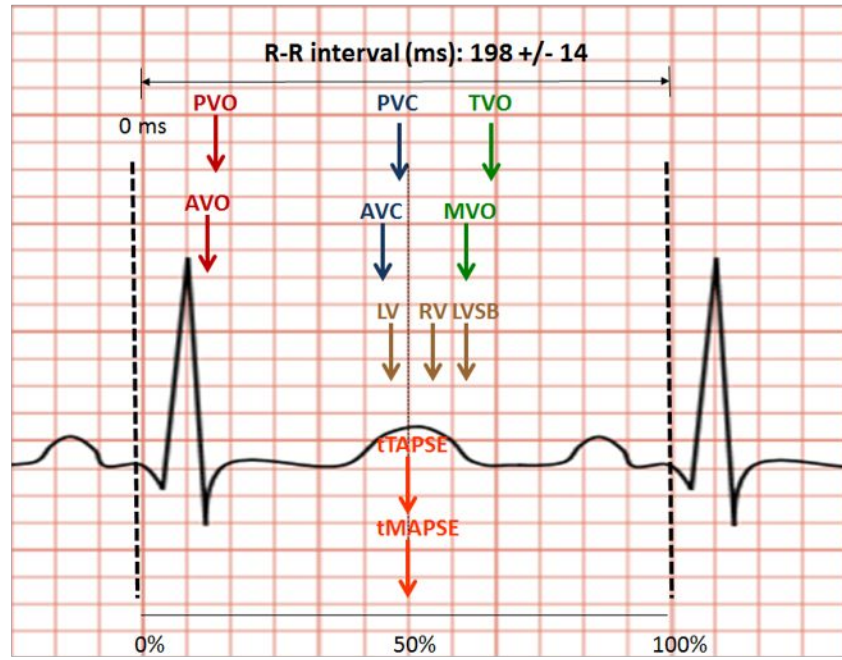

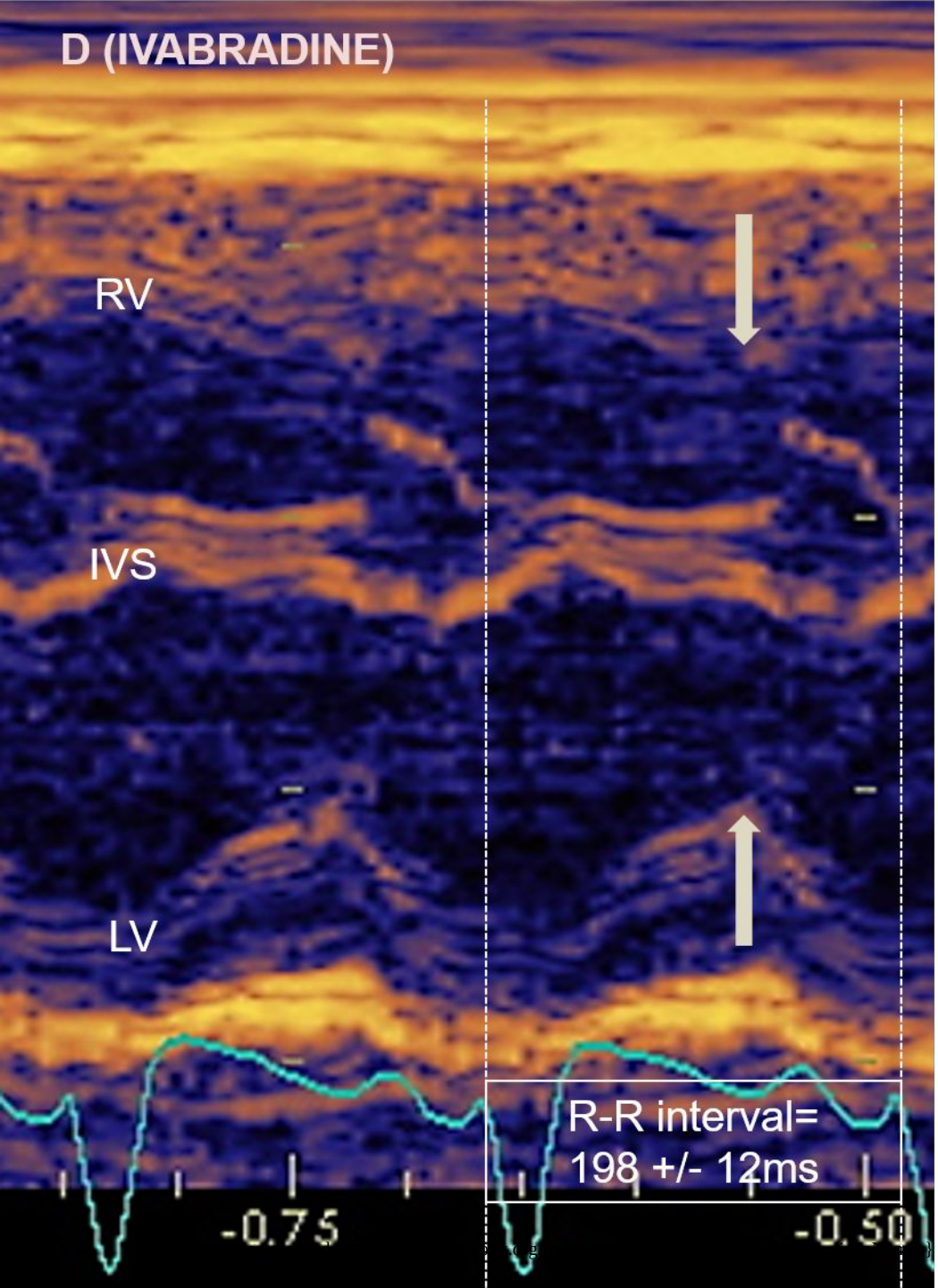


Figure 3 (D)

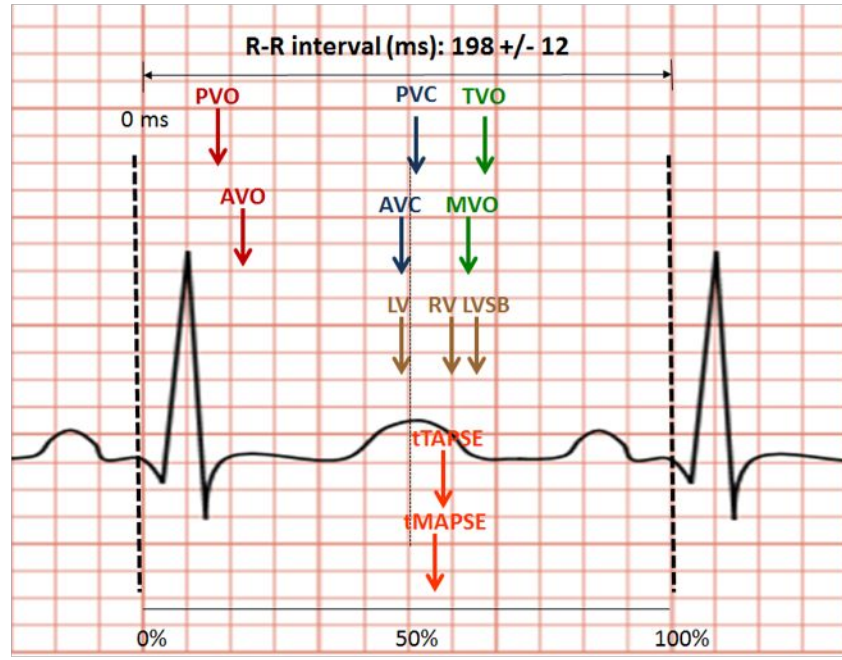

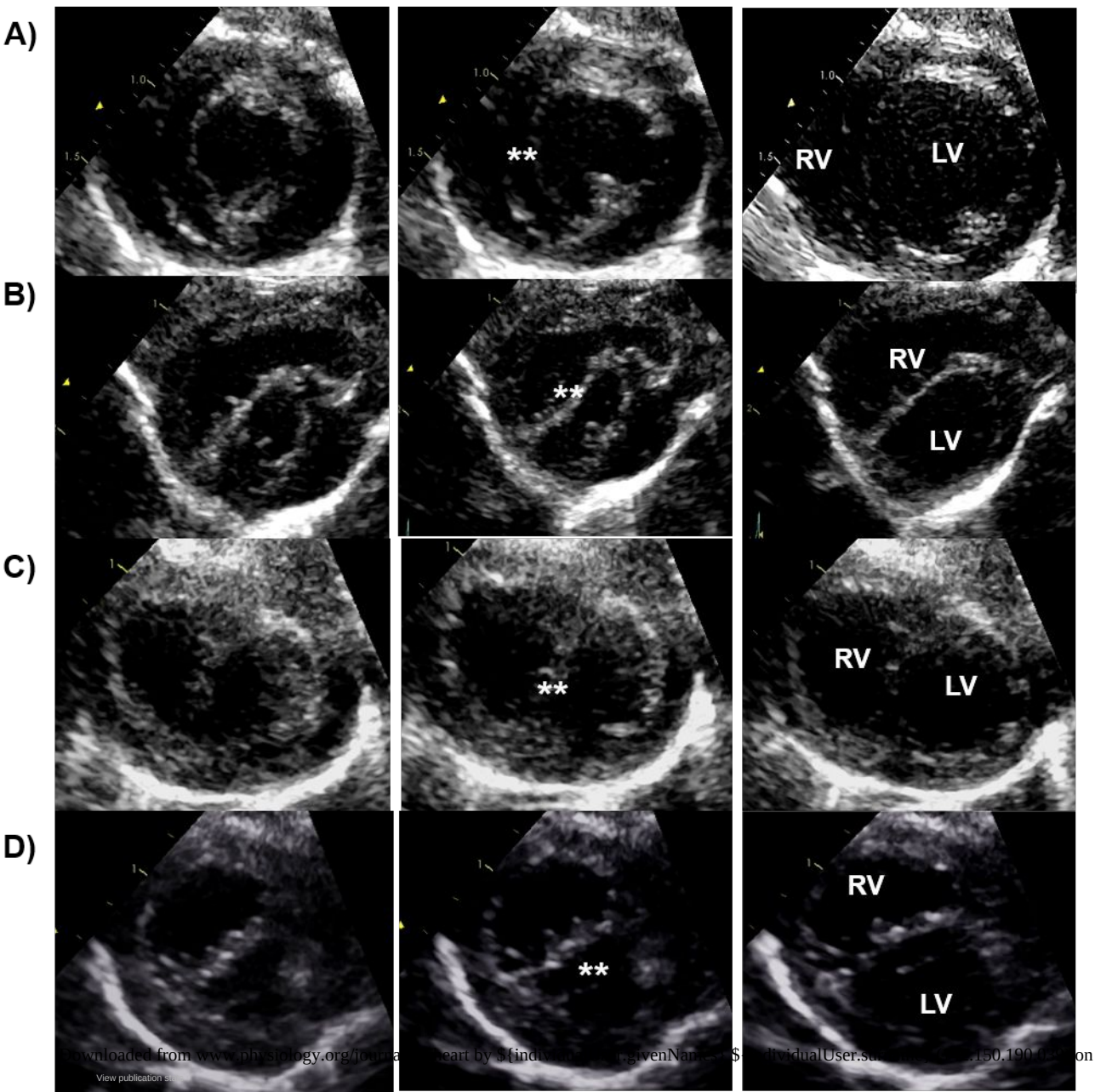


Figure 4